Article

Online System for Power Quality Operational Data Management in Frequency Monitoring Using *Python* and *Grafana*

Jose-María Sierra-Fernández [iD], **Olivia Florencias-Oliveros** [iD], **Manuel-Jesús Espinosa-Gavira,**
Juan-José González-de-la-Rosa *[iD], **Agustín Agüera-Pérez** [iD] and **José-Carlos Palomares-Salas** [iD]

Department of Automation Engineering, Electronics, Architecture and Computers Networks, Research Group
PAIDI-TIC-168, University of Cádiz, E-11202 Algeciras, Spain; josemaria.sierra@uca.es (J.-M.S.-F.);
olivia.florencias@uca.es (O.F.-O.); manuel.espinosa@uca.es (M.-J.E.-G.); agustin.aguera@uca.es (A.A.-P.);
josecarlos.palomares@uca.es (J.-C.P.-S.)
* Correspondence: juanjose.delarosa@uca.es

Abstract: This article proposes a measurement solution designed to monitor the instantaneous frequency in power systems. It uses a data acquisition module and a GPS receiver for time stamping and traceability. A *Python*-based module receives data, computes the frequency, and finally transfers the measurement results to a database. The frequency is calculated with two different methods, which are compared in the article. The stored data is visualized using the *Grafana* platform, thus demonstrating its potential for comparing scientific data. The system as a whole constitutes an efficient, low-cost solution as a data acquisition system.

Keywords: big data; data acquisition; data visualization; data exchange; dashboard; frequency stability; *Grafana*-based lab; power quality; GPS reference; frequency measurement

1. Introduction

The static and dynamic characterization of power systems is essential in order to assess the quality of the electricity supply (Power Quality, PQ). One of the most critical parameters is frequency, since its stability has a decisive influence on the operation of electrical machines. Special mention requires those that operate in synchronized mode, for which the deviations that occur with respect to their nominal value required for correct operation, are inadmissible [1].

As the characteristic parameters of the network can oscillate within a permitted range without being inappropriate for the equipment, it is essential to monitor whether they fall within these limits. In fact, in reality, the European frequency (50 Hz) is quite unstable, since the delivered signal is not perfectly sinusoidal, its admissible limits being 50 ± 0.1 Hz for systems with synchronous connection and 50 ± 2 Hz for isolated networks. [2–4].

Frequency shifts depend on a number of external factors. Common causes are light-ning strikes, connection and disconnection of huge loads, nonlinear loads, and groundings or short circuits in transmission lines [2]. Some well-known solutions have been developed to track the frequency, based on multiple procedures, for instance Zero Crossing (ZC) methods, Quadratic Forms (QF), Demodulation, Discrete (Fast) *Fourier* Transform (DFFT) with Phase Compensation (PC), etc. [3].

However, in the modern and increasingly intelligent electrical network (smarter grid) there are numerous distributed resources that, although a priori independent, require synchronized monitoring in order to evaluate the mutual influence and the global effect of their connection in the network. In response to this need, ad hoc measurement equipment was developed, the most relevant being the phasor measurement units (PMUs) [5–10].

PMUs are used to estimate the magnitude and phase of electrical magnitudes (e.g., voltage or current) [6–11]. Synchronization features are provided via GPS or IEEE 1588

Precision Time Protocol (PTP), designed to allow real-time synchronization of several remote points in the grid. PMUs capture samples of the power line signal and rebuild the so-called phasor quantity (magnitude and phase), which constitutes the mathematical model of the waveform under test. The result is a time-synchronized measurement quantity known as syncrophasor [10,11].

PMUs are capable of detecting abnormal waveform shapes. For instance, if both supply and demand do not match perfectly, the associated frequency imbalances cause "tightness" within the grid, which is a potential cause for power outages. PMUs are also designed to measure the frequency in the power grid. Indeed, a typical commercial PMU can report measurements with very high temporal resolution, up to 120 measurements per second (30, 60 and 120 are common reporting rates) [10]. This helps with analyzing dynamic events in the grid, which is not possible with traditional SCADAs that generate one measurement every 2 or 4 s. Therefore, PMUs with enhanced monitoring and control capabilities are considered as one of the most important measuring devices in the current and future design of power systems [7–12].

Besides the high prices (the average overall cost per PMU—the cost for procurement, installation and commissioning—ranges from USD 40,000 to USD 180,000), in most cases PMUs measure the voltage magnitude and the phase angle, assuming that the frequency remains constant [6]. This starting hypothesis is precisely disregarded in PMU's indirect measurements. These operations are essentially based on the formulation of a mathematical problem whose purpose is to fit the measurements to a sinusoidal curve. Consequently, when the sinusoidal curve is not ideal, the PMU fails to make exactly that adjustment. In this way, the less sinusoidal the voltage supply signal, the worse the adjustment made and the lower the quality of the phasor generated. This situation is very common in the modern grid, in which distributed and random generation, and the presence of nonlinear loads, make it necessary to adopt new strategies in order to complement the existing ones based on PMUs [13,14].

Considering all of the above, the present work proposes a monitoring solution for the frequency of the electrical network (grid frequency), which is complementary to the existing ones, based on PMUs, in the following double sense that constitutes the core essence of the contribution of this work. On the one hand, it provides a more precise frequency measure, based on the Allan variance, and thus contributes to the enhancement of the characterization of the network. On the other hand, the system is capable of managing large volumes of data (big data) that flood the electrical network [15], allowing the user to extract the necessary information at all times for a better and less subjective way of understanding the energy management and quality of the supply (PQ).

The instrument hardware is based on the GPS receiver-data acquisition (DAQ) system binomial; the latter driven by a computer program developed in *Python*. The first one provides traceable time stamping, with the help of the 1 pulse per second (PPS) signal, and a precision of 1 ppm. In this way, the developed system adapts to what is established in the PQ regulatory framework [2], obtaining frequency values every 10 s, with a temporal resolution better than 20 ms [5,6], minimizing delays associated with heavy software diagrams and programming codes.

Another proposal and challenge of the present work is the use of *Grafana* as a visualization tool for massive data related to the quality of the supply, and specifically to the frequency of the network. The work is part of an emerging trend of development of low-cost data acquisition frameworks, which often constitute alternative solutions and complementary functionalities to those offered by SCADAs [9]. Commercially named *PyFreqDAQ*, this DAQ-F system incorporates an easy-to-use graphical user interface, allowing a simple control and automation of a huge variety of experimental setups for frequency measurement.

This is the motivation of the work and the general context of the research. The rest of the paper is structured as follows. Section 2 provides details regarding the system description and arrangement. Then, in Section 3, *PyFreqDAQ* operation is detailed along with the frequency calculation. Section 4 displays and explains graphical results of data analysis from *Grafana*. Finally, conclusions are drawn in Section 5.

2. System Description and Arrangement

From here onwards, the proposed distributed instrument will be described. The hardware consists essentially of a chassis and a data acquisition card (DAQ) from the manufacturer NI™, which receives, on the one hand, the voltage input (50 Hz, 220 V_{rms}) from the electrical network and, on the other, the pulsed signal (1 PPS) from the GPS receiver (Symmetricon™) disciplined clock. The pulses of the latter are used as traceable references for time domain stamping and as references to calculate the frequency according to the Allan variance (Figure 1). The data are transferred from the acquisition card to the computer via Ethernet. Later, they are processed, and the processing results transferred to the database. All this is performed by software programmed in *Python*. Using these data, it is possible to graph the evolution of the frequency in the required time interval, in order to carry out the monitoring of the electrical network [13].
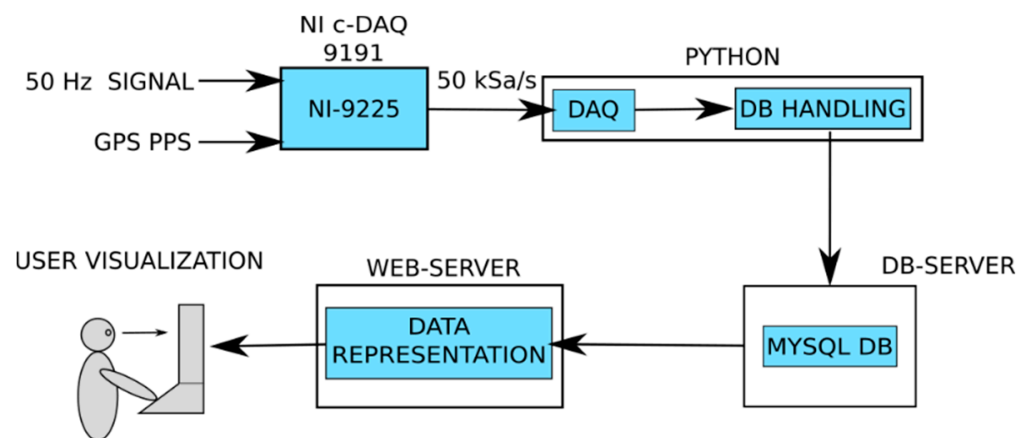

Figure 1. System block diagram. The c-DAQ module acquires the signals and transfers the information to online software. It saves information in the DB and then data is represented on an online viewer.

The monitoring solution developed according to this strategy allows for obtaining data from multiple measurement sources, and putting them in common in a database, which is available on the display. With this, since a large amount of signal data from different points can be observed and analyzed (compared), the maintenance of the network can be carried out using spatial and temporal compression strategies, which offer a simplified and truthful statistical vision of the huge amount of initial data (big data).

In order to obtain an overview of the measurement solution, Figure 1 shows a block diagram, which indicates the direction of the signal flow and the interactions between the different elements that make up the system.

The *PyFreqDAQ* measurement chain consists of a GPS receiver for the synchronization, a plug connected to the network responsible for acquiring the signal, and a DAQ card that receives both signals and sends them to the PC. This can be seen in detail in Figure 2.
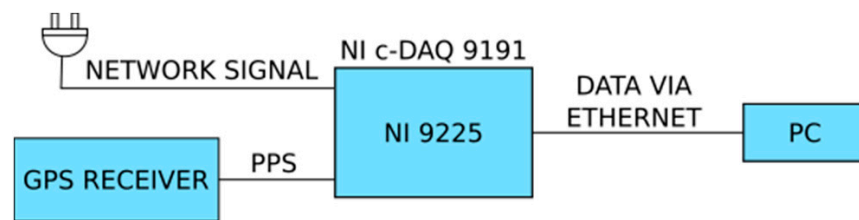
Figure 2. Scheme of the measurement chain. Network signal and GPS-PPS signal are acquired with the DAQ card (NI 9225) inside the chassis (c-DAQ-9191). It processes them and sends data to the PC via Ethernet.

Figure 3 shows the connections of the GPS-PPS and the voltage signals to the card NI 9225 (simultaneous, channel-to-channel isolated). This three-channel module allows up to 300 V_{rms}, with a sampling frequency of 50 kS/s and 24 bits. Data are used to calculate frequency later. The card NI 9225 is allocated inside the chassis NI 9191. The chassis controls timing, synchronization and data transfer between I/O modules and the external server.

Figure 3. The NI 9225 card inside the chassis cDAQ-9191 (1-Slot, Ethernet and 802.11 Wi-Fi compact DAQ chassis) with wiring connections: Yellow wires ("crocodile"-type probes) correspond to the GPS-PPS signal while the black-covered wires brings the network voltage signal directly by connecting to it with a plug.

The equipment, model Symmetricom™ TrueTime XL-AK GPS synchronized receiver, assures ultraprecise time and frequency delivery. This configurable piece of instrument provides timing outputs within 40 ns of UTC/USNO and frequency outputs accurate to less than 1×10^{-12}. It includes 1 PPS output that provides a reference for the frequency calculation using the Allan variance.

For data processing, calculations, as well as sending information to the database, two *Python* software projects are constantly running in parallel. The first one is responsible for receiving data transmitted from the NI 9225, calculating frequency and sending the results to the second one. First project is referred to as "DAQ"; the second project being responsible for receiving data from the DAQ and organizing it within the database. This part is referred to as "DB handling". Figure 4 shows, in a simplified way, the workflow of the projects, and Figure 5 shows the *Python* codes associated with data acquisition.
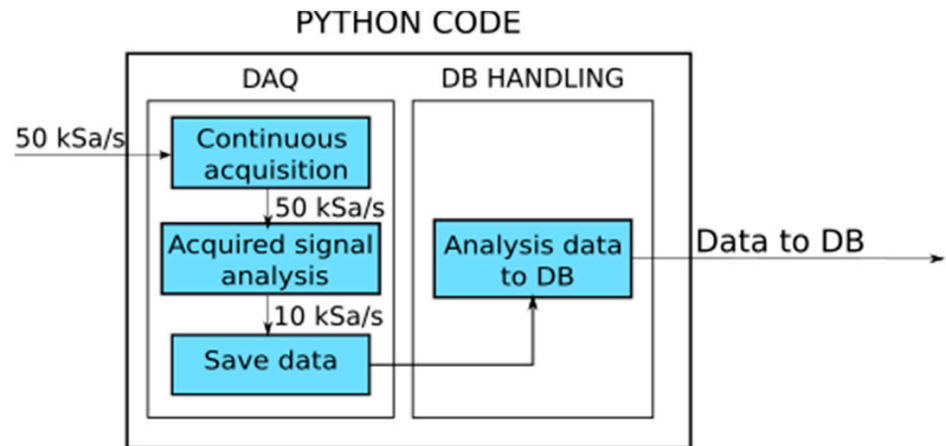
Figure 4. *Python* code operation with the two projects. Data is registered at 50 kSa/s and received by the first project, *DAQ*, responsible for acquiring and transferring to the second project at a rate of 10 kS/s. The second project, *DB Handling*, stores them and manages the database.

Finally, data is represented on *Grafana*, a well-known, multiplatform, open-source analytics and interactive visualization web application. It provides charts, graphs, and alerts for the web when connected to supported data sources. As a visualization tool, *Grafana* is a very popular component in monitoring stacks, often used in combination with time series databases and monitoring platforms. In this work, it allows for user data surveillance.

```python
with nidaqmx.Task() as readTask:

    for i_device in range(len(devices_hosts)):
        device = nidaqmx.system.device.Device(device_names[i_device])

        try:
            device.add_network_device(devices_hosts[i_device], device_name=device_names[i_device],
                                      attempt_reservation=True, timeout=10.0)
        except Exception as e:
            print(e.__str__())
        try:
            device.reserve_network_device(override_reservation=True)
        except Exception as e:
            print(e.__str__())

    for channel in list_chanel:
        readTask.ai_channels.add_ai_voltage_chan(channel)

    readTask.timing.cfg_samp_clk_timing(rate=sampleRate,
                                        sample_mode=nidaqmx.constants.AcquisitionType.CONTINUOUS,
                                        samps_per_chan=readNumber)

    reader = AnalogMultiChannelReader(readTask.in_stream)

        """Reading data from the buffer in a loop. """
        output = np.zeros([list_chanel.__len__(), readNumber])

        readTask.start()
        base = datetime.datetime.now()  # get time at measurement start
        dT = 1 / sampleRate
        dT_meas = round(dT * readNumber)  # time among measures in us
        base1 = base - datetime.timedelta(
            seconds=dT_meas)
        # calculates time at a measurement interval before start, to create a reference time vector
        # now, create a reference time vector, from previous time interval.
        t = np.array([base1 + datetime.timedelta(seconds=dT * i) for i in range(readNumber)], dtype='datetime64')

        flag_countinue_acqsition = True
        while flag_countinue_acqsition:
            reader.read_many_sample(data=output,
                                    number_of_samples_per_channel=readNumber, timeout=timeoutRead)
            t_ant = t  # save t as t_ant, as reference
            t = t_ant + np.timedelta64(dT_meas, 's')  # increment time vector in time among measurements
            for i_data in range(output.shape[0]):
                output[i_data] = output[i_data] * scales[i_data]
            try:

                queue.put([t, output], timeout=2)

            except Exception as e:

                print(e.__str__())
                print('Error  acquisition')

                flag_countinue_acqsition = False
            if not stop_queue.empty():
                flag_countinue_acqsition = False

        readTask.stop()
        print('Acquisition Stop')
```

Figure 5. The *Python* code associated with data acquisition project.

3. *PyFreqDAQ* Operation and Frequency Calculation

The card NI 9225 receives data from two inputs (sampling frequency is 50 kS/s): the voltage line signal by connecting directly to a wall plug, and the GPS-PPS signal that allows an absolute time reference. Raw data are then transferred via Ethernet to the software running on the PC.

The first of the two projects, referred to as "DAQ", is constantly reading signal data acquired from the NI 9225. Calculations are performed in two ways. The PPS is used for the calculations contemplating the theoretical frequency of 50 Hz, so each theoretical cycle lasts 20 ms.

The voltage line is driven to a *Schmitt* trigger in order to be conditioned (it returns a square waveform with the same frequency as the input signal). When the input voltage is higher than a chosen upper threshold, the output is high, and when the input falls below a lower level, the output is low. If the input voltage is between both thresholds, the output remains in the same previous state (Figure 6). Then, calculations can be performed by fragmenting this square waveform into its cycles.
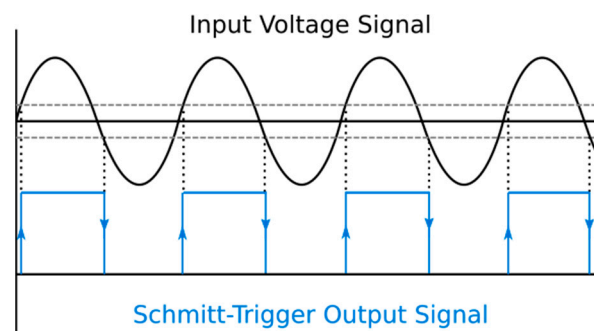

Figure 6. *Schmitt*-trigger effect produced with the input voltage signal. The input voltage signal is drawn as a black sinus and the output signal is the blue square signal. Scales and units are omitted for simplicity.

Between every two pulses coming from the GPS (1 PPS signal), complete periods of the signal boxed by the *Schmitt*-trigger can be found, as well as part of them, which have been interrupted by the 1 PPS signal. The sum of all of them must be equal to one second. Figure 7 shows an example of this circumstance that shows the exact behavior of the signal processing.
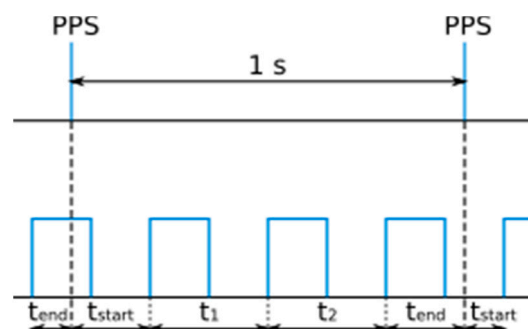

Figure 7. *Schmitt*-trigger output signal chopped by the 1 PPS pulses. This allows for measuring the signal phase and the Allan Variance.

For those cycles that contain a GPS-PPS signal, the phase is measured, bearing in mind that each cycle corresponds to a phase shift of $360°$. The next two illustrations, Figures 8 and 9, show the real PPS signal from the GPS receiver and *Schmitt*-trigger signals, at different sampling rates, from the lab oscilloscope.
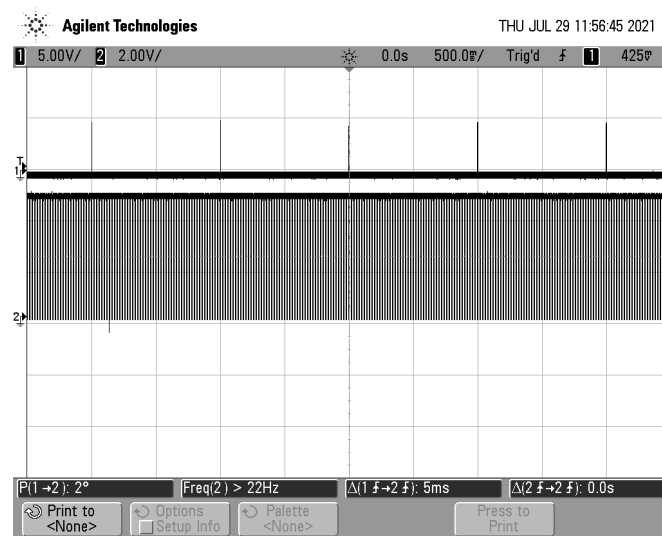
Figure 8. *Schmitt*-trigger output signal and PPS pulses. Five PPS pulses can be seen at the top while the total of the cycles are monitored in the signal below.
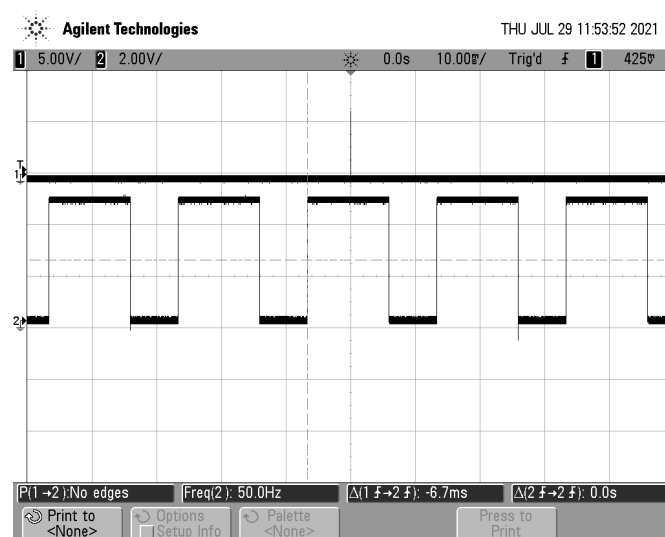
Figure 9. *Schmitt*-trigger application result for the input voltage signal. In this sample only 1 PPS is seen, but the square signal from the Smith-trigger is clearly observed.

Using the signal phase, hereinafter Allan variance is calculated. It has exhibited efficient performance in frequency stability characterization of precision sources in authors' previous works [13]. Furthermore, frequency. The first parameter to be considered in the computation scheme is known using the Allan variance, we can calculate frequency using frequency deviation from a reference as the fractional frequency deviation:

$$y(t) = \frac{f(t) - f_0}{f_0} \tag{1}$$

This depends on the actual frequency and the base frequency, f_0. In this case, f_0 corresponds to the ideal network frequency of 50 Hz. It is calculated by the deviation from the actual frequency with respect to f_0, in a relative or fractional form.

Time deviation is also calculated, starting from the base frequency. At an instant t, the signal advances a phase of $\phi(t)$. If the frequency was equal to the base one:

$$\phi(t) = 2\pi f_0 t \tag{2}$$

So, if $\phi(t)$ is divided by $2\pi f_0$, and the frequency is ideal, it would result "t". Then, if we subtract "t" from that fraction, time deviation can be obtained for an instant t but also instant t + 1:

$$x(t) = \frac{\phi(t)}{2\pi f_0} - t \tag{3}$$

So far, as each increment of +1 corresponds to an increment of τ in time, it can be determined as a fractional time increment, which would be equal to the frequency increment:

$$
\begin{aligned}
\bar{y}_k &= \frac{1}{\tau}(x_{k+1} - x_k) \\
&= \frac{1}{\tau}\left(\left(\frac{\phi_{k+1}}{2\pi f_0} - t(k+1)\right) - \left(\frac{\phi_k}{2\pi f_0} - t(k)\right)\right) \\
&= \frac{1}{\tau}\left(\frac{\phi_{k+1} - \phi_k}{2\pi f_0} - t(k+1) + t(k)\right) = \frac{1}{\tau}\left(\frac{\Delta\phi}{2\pi f_0} - \tau\right)
\end{aligned}
\tag{4}
$$

The phase increment is computed using the start and ending phases, before and after the PPS signal:

$$\phi_{end} = 2\pi \cdot \frac{t_{end}}{t_{start} + t_{end}} \tag{5}$$

$$\phi_{start} = 2\pi \cdot \frac{t_{start}}{t_{start} + t_{end}} \tag{6}$$

Additionally, with them, the phase increment of each second is:

$$\Delta\phi = \phi_{start} + 2\pi N + \phi_{end}, \tag{7}$$

N being the number of cycles. All in all, the instantaneous frequency at instant t for the kth-measure obeys the following equation:

$$\frac{\bar{f}_k}{f_0} - 1 = \bar{y}_k; \quad \frac{\bar{f}_k}{f_0} = \bar{y}_k + 1; \quad \bar{f}_k = f_0(\bar{y}_k + 1) \tag{8}$$

Expression of $\bar{y}_k$ from Equation (4) is replaced in Equation (8):

$$\bar{f}_k = f_0\left(\frac{1}{\tau}\left(\frac{\Delta\phi}{2\pi f_0} - \tau\right) + 1\right) \tag{9}$$

If $\tau = 1$, we have:

$$\bar{f}_k = f_0\left(\frac{1}{1}\left(\frac{\Delta\phi}{2\pi f_0} - 1\right) + 1\right) = f_0\frac{\Delta\phi}{2\pi f_0} = \frac{\Delta\phi}{2\pi} \tag{10}$$

$\Delta\phi$ is then replaced using Equation (7):

$$\bar{f}_k = \frac{\phi_{start_{ant}} + 2\pi N + \phi_{end}}{2\pi} \tag{11}$$

Splitting into simple fractions and replacing ϕ_{start} and ϕ_{end} by their expressions in Equations (5) and (6) yields:

$$\bar{f}_k = \frac{t_{start_{ant}}}{t_{start_{ant}} + t_{end_{ant}}} + N + \frac{t_{end}}{t_{start} + t_{end}} \tag{12}$$

As is observed in Figure 6, t_{start} is the time elapsed from the initial PPS to the end of the cycle which is broken by this pulse, and t_{end} is the time elapsed from the beginning of the last cycle (considered between the two PPS) and the final PPS.

The frequency is calculated according to two different methods. On the one hand, a specific method is used in which the frequency and its associated uncertainty are calculated

every second using the method based on Allan variance. On the other hand, a traditional method has been used, regulated in accordance with the UNE 50160 standard, which calculates the frequency every 10 s.

Once the calculations are performed, data results are transferred to the second *Python* project (DB handling). This project is responsible for saving and organizing MySQL database, with the aim of being rapid. *Grafana* obtains data directly from the database and represents it with timescales and other resources so that the user can visualize the evolution of the variables.

4. Results

The database is organized according to different tables. If necessary, the information could be stored in the same table, but this would lead to very heavy data matrices, which would slow down the search engine, and consequently all the operations derived from it would entail a high computational cost. To emphasize this size, putting the focus on the Allan frequency, which is the most loading case of the two measurement strategies compared in this work, one result is sent to the database every second, resulting in 86,400 rows generated per day; 604,800 per week; in one month, 18,748,800 and in one year 31,536,000. To solve the above-mentioned big-data issues, this is programmed directly by the *DB handling*, for both Allan and regulated frequencies. As examples, Tables 1 and 2 show the measurements corresponding to the month of May. Each table preserves its original design in order to show a *Grafana* perspective.

Table 1. Allan frequency table (offline measurements) for one month, extracted from *Grafana* database. It keeps its original format.

id	absolute_signal_id	time	frequency
1	19997	2021-05-03 08:50:47	50.0099
2	19998	2021-05-03 08:50:48	49.9878
3	19999	2021-05-03 08:50:49	50.0263
4	20000	2021-05-03 08:50:50	50.0701
5	20001	2021-05-03 08:50:51	49.9916
6	20002	2021-05-03 08:50:52	50.0064
7	20003	2021-05-03 08:50:53	49.9766
8	20004	2021-05-03 08:50:54	49.9205
9	20005	2021-05-03 08:50:55	50.0115
10	20006	2021-05-03 08:50:56	50.0458
11	20007	2021-05-03 08:50:57	50.0317
12	20008	2021-05-03 08:50:58	49.972
13	20009	2021-05-03 08:50:59	50.013
14	20010	2021-05-03 08:51:00	49.9837

Table 2. Frequency measurements (according to norm 6100-4-30) table extracted from *Grafana*.

id	absolute_signal_id	time	frequency
28	20287	2021-05-03 08:55:36	49.9691
29	20297	2021-05-03 08:55:46	50.0106
30	20307	2021-05-03 08:55:56	50.0015
31	20317	2021-05-03 08:56:06	49.9994
32	20327	2021-05-03 08:56:16	49.994
33	20343	2021-05-03 08:56:36	50.0048
34	20354	2021-05-03 08:56:56	50.0047
35	20437	2021-05-03 09:43:16	49.9988
36	20447	2021-05-03 09:43:26	49.9955
37	20457	2021-05-03 09:43:36	50.0053
38	20467	2021-05-03 09:43:46	50.003
39	20477	2021-05-03 09:43:56	50.0082
40	20487	2021-05-03 09:44:06	49.9825
41	20497	2021-05-03 09:44:16	50.0116

It can be verified that one frequency datapoint has been generated each second just looking at the "time" column.

Additionally, it can be verified that frequency is registered in 10-second periods, as is stated. In both tables there are four columns, labeled: "id", "absolute signal id", "time" and "frequency". "id": primary key of the correspondent table, autoincrement, serves to enumerate the rows of the monthly table. "Absolute signal id": foreign key from the global signal list table. "Time": date in which the measurement was taken. Format: YYYY-MM-DD HH:MM:SS. "Frequency": calculated frequency value in Hz. Following these critera, it is faster to make the queries that are aligned with *Grafana*. Indeed, *Grafana* uses data stored in tables for implementing the desired graphics. The graphics are called "Dashboards" and the users can create as many as desired using available data [15].

The platform is capable of selecting data from the tables according to certain search criterion. For example, in the present work, for the sake of representing the evolution over time of frequency values, the table of a specific month for a specific time interval to be represented can be selected. In this case, the platform extracts only the columns of time and frequency from the tables.

The standard UNE-EN 50160:2011 establishes the limits that the frequency cannot overtake, and mentions that the frequency has to be measured using 10-s periods [2]. Figure 10 shows the evolution of the frequency over 15 min, measured as indicated by the norm.
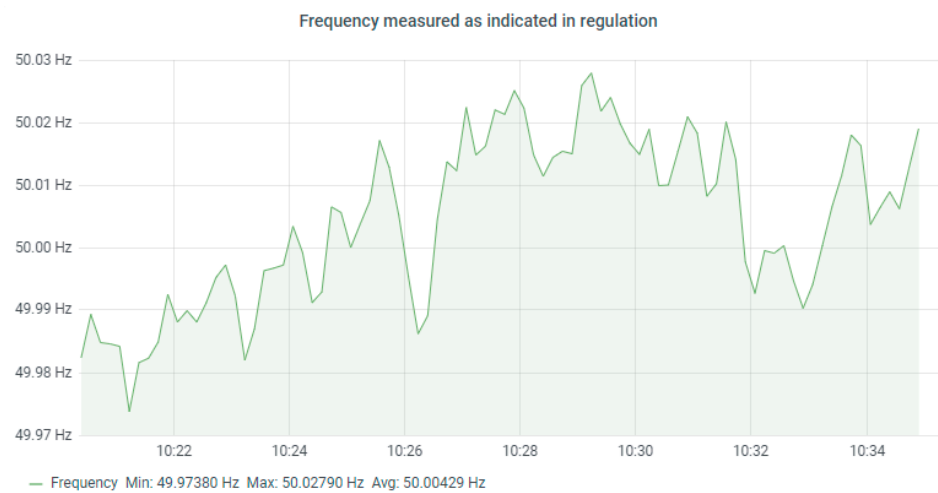
Figure 10. Evolution of the measured frequency (vs. time) following the norm, with values each 10 s, over 15 min.

To study the difference between the two frequency calculation methods, the following dashboard on *Grafana* compares the evolution of both frequencies. A time interval of 15 min has been chosen, as can be observed in Figure 11.
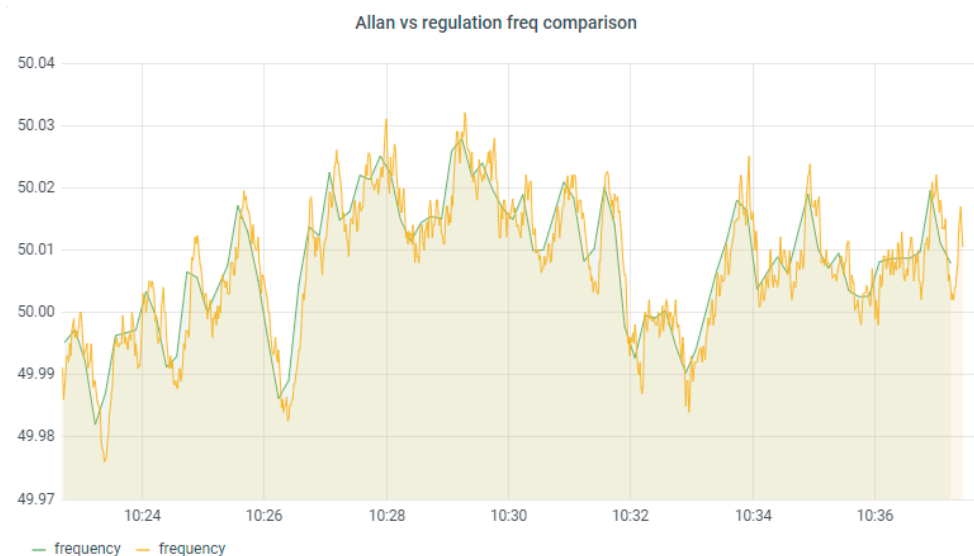

Figure 11. *Frequency timeline following* the regulation (green line) and following the algorithm using Allan Variance (orange line).

Looking at Figure 11, the difference between the results the two methods is clear. First, the evolution of frequency measured by the regulation method looks softer than the other one. The reason is clear; with the method that establishes the regulation, the frequency calculation is conducted for periods of 10 s, so one measure is available for each 10 s. With the Allan algorithm, frequency is calculated each second, so the number of measures available is 10 times greater, thus there is a tendency for a lot of peaks compared to the other one.

In addition to this, Allan frequency is totally synchronized thanks to the GPS-PPS signal, so it can be stated that this method is more accurate that the one that regulation establishes.

Observing the measures over time, it has been proven that frequency did not exceeded the established limits for at least 10 s, in which case, frequency would be out of what current

regulation dictates. A *Grafana* a heat-map showing the distribution of Allan frequency through time is also presented (Figure 12).
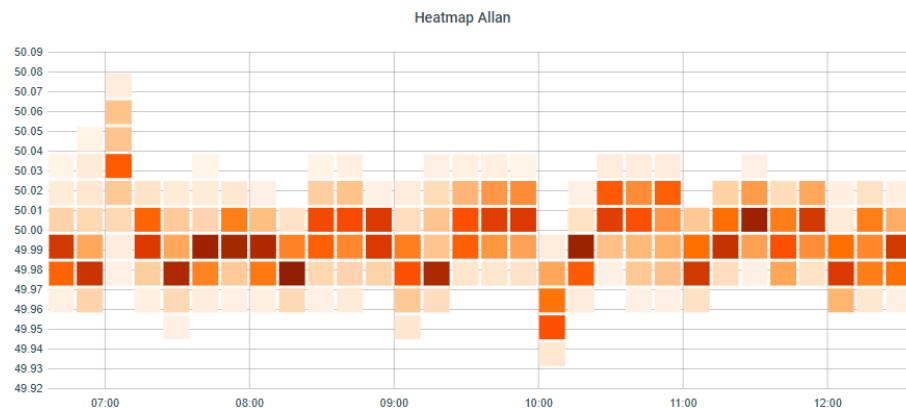

Figure 12. Heatmap of Allan-based frequency measurements.

The horizontal axis corresponds to the timescale. Figure 12 is divided into one-hour intervals. Each interval contains five columns of squares, so each column corresponds to an interval of twelve minutes. The vertical axis corresponds to the frequency scale. As the Allan frequency is measured each second and each square in column corresponds to twelve minutes, for each column we have 720 measurements. To indicate the distribution of these measurements, in each column there are various squares of different colors. The darker the square, the more measurements have been recorded within the considered frequency interval. It can be observed that data continuously fluctuate around 50 Hz. The rest of the measurements are assumed to be outliers, as observed in fluctuations that fall outside the frequency range of 49.95–50.03 Hz, approximately.

5. Conclusions and Future Work

In this work, a low-cost measurement solution (called *PyFreqDAQ*) has been proposed to monitor the frequency of the electrical network, considered as a quality parameter of the electrical supply, and at the same time offer a more precise result thanks to the use of the Allan variance. The hardware is managed by *Python*, and open-source software (*Grafana*) is available that allows for monitoring the evolution of the frequency, in order to study the limits between which it is maintained. This measurement solution is original in that it does not use high-level visual programming software for data acquisition and data management (e.g., labVIEW™), thus lightening the computational load, an issue that could be the subject of future work.

In order to show its operating power, the frequency has been calculated according to two different methods. The first is in accordance with the regulations of the IEC 61000-4-30 standard. The second uses an algorithm that provides the measured frequency with greater precision and a reference traceable via GPS, which is the Allan variance-based algorithm.

Among the many benefits of the Allan variance-based method it is worth citing its better precision, lower error, faster calculations, and a wider range of measurements available to users.

The use of *Python* to program the data acquisition card and manipulate the database has shown much greater flexibility than other applications (e.g., labVIEW™). In effect, Python is a more powerful programming language, and consequently, it allows operations and calculations to be carried out using simple codes, while allowing for a low computational load and consuming much less working memory. In future works, a *Python* vs. labVIEW™ comparative could be studied, which would be unique research, to date.

All in all, the joint use of *Python* and *Grafana* to receive and process, perform operations on and visualize the data, has proven to be very efficient in the sense of perfectly adapting

to the regulations and at the same time offering a flexible measurement solution, which is adapt to the modern and smart electrical grid.

Finally, the emerging *Grafana* monitoring solution in the field of distributed instrumentation, not considered to date in power-supply quality studies, allows for a much easier visualization of the data within a web environment. In future works, the performance of *Grafana* against other web programming environments should be compared for a monitored variable, which could be the frequency of the network or the industrial frequency. Research could look at comparing computation times, flexibility and ease of choice of the variables to be displayed. Indeed, with *Grafana* and the measurement platform developed by simply choosing a set of parameters and connecting them to the database, the visualization is interactive and immediate, constituting a simple task that requires little time, that can be carried out by an operator plant with a very basic training.

Author Contributions: J.-M.S.-F. and M.-J.E.-G. programmed *Phyton* codes. O.F.-O. and J.-J.G.-d.-l.-R. developed the whole paper organization and were responsible for experiments design and equipment operation. A.A.-P. and J.-C.P.-S. analyzed and interpreted graphs in the frame of comparison the two methods of frequency measurement. All authors have read and agreed to the published version of the manuscript.

References

1. Thomas, D.W.P.; Woolfson, M.S. Evaluation of frequency tracking methods. *IEEE Trans. Power Deliv.* **2001**, *16*, 367–371. [CrossRef]
2. IEC 61000-4-30:2015. *Electromagnetic Compatibility (EMC). Part 4-30: Testing and Measurement Techniques—Power Quality Measurement Methods*; IEC: Geneva, Switzerland, 2015.
3. Moreno-Muñoz, A.; Sánchez, J.A.; de la Rosa, J.J.G.; Luna, J.J. Application of smart sensors to the measurement of power quality. In *Conference Record—IEEE Instrumentation and Measurement Technology Conference*; 2008; pp. 218–222. Available online: https://www.researchgate.net/publication/4343132_Application_of_smart_sensors_to_the_measurement_of_power_quality (accessed on 7 December 2021).
4. Melo, I.D. Harmonic state estimation for distribution systems based on optimization models considering daily load profiles. *Electr. Power Syst. Res.* **2019**, *170*, 303–316. [CrossRef]
5. Golsorkhi, M.S.; Savaghebi, M.; Lu, D.D.C.; Guerrero, J.M.; Vasquez, J.C. A GPS-based control framework for accurate current sharing and power quality improvement in microgrids. *IEEE Trans. Power Electron.* **2017**, *32*, 5675–5687. [CrossRef]
6. US Department of Energy. *Factors Affecting PMU Installation Costs*; 2014. Available online: https://www.smartgrid.gov/files/recovery_act/PMU-cost-study-final-10162014_1.pdf (accessed on 7 December 2021).
7. de Oliveira, B.C.; Melo, I.D.; Souza, M.A. Bad data detection, identification and correction in distribution system state estimation based on PMUs. *Electr. Eng.* **2021**, 1–17. [CrossRef]
8. Zhou, W.; Ardakanian, O.; Zhang, H.-T.; Yuan, Y. Bayesian Learning-Based Harmonic State Estimation in Distribution Systems with Smart Meter and DPMU Data. *IEEE Trans. Smart Grid* **2020**, *11*, 832–845. [CrossRef]
9. Kusic, G.L.; McGahey, W.E.; Lehtonen, M. Measurement of power system phase differences by means of GPS timing. In Proceedings of the 10th International Conference—2016 Electric Power Quality and Supply Reliability, PQ 2016, Tallinn, Estonia, 29–31 August 2016; pp. 297–300.

10. Thakre, M.; Ahmad, A.; Bhadane, K. Measurement Class Phasor Measurement Unit Compliance for Electrical Grid Monitoring. *MAPAN-J. Metrol. Soc. India* **2021**, 1–11. [CrossRef]

11. Abdullah-Sufyan, M.A.; Zuhaib, M.; Anees, M.A.; Khair, A.; Rihan, M. Implementation of PMU-Based Distributed Wide Area Monitoring in Smart Grid. *IEEE Access* **2021**, *9*, 140768–140778. [CrossRef]

12. Pallarés-López, V.; Moreno-Muñoz, A.; Polonio-Torrellas, M.; Moreno-García, I.M.; González-de-la-Rosa, J.J. A experimental IEEE1588-BASED system for synchronized phasor measurement in electric substation. In Proceedings of the IEEE 2010 5th IEEE Conference on Industrial Electronics and Applications, Taichung, Taiwan, 15–17 June 2010.

13. González-de-la-Rosa, J.J.; Moreno-Muñoz, A.; Lloret, I.; Pallarés, V.; Liñán, M. Characterisation of frequency instability and frequency offset using instruments with incomplete data sheets. *Measurement* **2006**, *39*, 664–673. [CrossRef]

14. Florencias-Oliveros, O.; González-de-la-Rosa, J.J.; Agüera-Pérez, A.; Palomares-Salas, J.C. Power quality event dynamics characterization via 2D trajectories using deviations of higher-order statistics. *Measurement* **2018**, *125*, 350–359. [CrossRef]

15. Weber, S.J. PyMoDAQ: An open-source Python-based software for modular data acquisition. *Rev. Sci. Instrum.* **2021**, *92*, 045104. [CrossRef] [PubMed]